Pseudopotentials for quantum Monte Carlo studies of transition metal oxides

Jaron T. Krogel,[1] Juan A. Santana,[1] and Fernando A. Reboredo[1]

[1] *Materials Science and Technology Division, Oak Ridge National Laboratory, Oak Ridge, TN 37831, USA*

This manuscript has been authored by UT-Battelle, LLC under Contract No. DE-AC05-00OR22725 with the U.S. Department of Energy. The United States Government retains and the publisher, by accepting the article for publication, acknowledges that the United States Government retains a non-exclusive, paid-up, irrevocable, world-wide license to publish or reproduce the published form of this manuscript, or allow others to do so, for United States Government purposes. The Department of Energy will provide public access to these results of federally sponsored research in accordance with the DOE Public Access Plan (http://energy.gov/downloads/doe-public-access-plan).

Pseudopotentials for quantum Monte Carlo studies of transition metal oxides

Jaron T. Krogel,[1] Juan A. Santana,[1] and Fernando A. Reboredo[1]

[1] *Materials Science and Technology Division, Oak Ridge National Laboratory, Oak Ridge, TN 37831, USA*

(Dated: January 27, 2016)

Quantum Monte Carlo (QMC) calculations of transition metal oxides are partially limited by the availability of high quality pseudopotentials that are both accurate in QMC and compatible with major planewave electronic structure codes. We have generated a set of neon core pseudopotentials with small cutoff radii for the early transition metal elements Sc to Zn within the local density approximation of density functional theory. The pseudopotentials have been directly tested for accuracy within QMC by calculating the first through fourth ionization potentials of the isolated transition metal (M) atoms and the binding curve of each M-O dimer. We find the ionization potentials to be accurate to 0.16(1) eV, on average, relative to experiment. The equilibrium bond lengths of the dimers are within 0.5(1)% of experimental values, on average, and the binding energies are also typically accurate to 0.18(3) eV. The level of accuracy we find for atoms and dimers is comparable to what has recently been observed for bulk metals and oxides using the same pseudpotentials. Our QMC pseudopotential results also compare well with the findings of previous QMC studies and benchmark quantum chemical calculations.

PACS numbers: 71.10.-w, 71.15.-m, 71.15.Dx, 71.15.Nc

Transition metal oxides are an essential class of materials for energy applications. These materials find applications as diverse as catalysis, energy storage, and superconductivity. The ability to tailor the electronic functionality of transition metal oxides is clearly bolstered by continuing to develop a detailed theoretical understanding of these materials. Unfortunately it is this same class of materials that presents some of the greatest resistance to detailed theoretical characterization. Part of this challenge directly relates to the more localized electrons occupying the partially filled d states of the transition metal cations, leading to strong electron-electron interactions. Early characterizations of transition metal oxides by band theory incorrectly predicted many of them to be metals[1]. This departure from the expectations of band theory has lead to the widespread acceptance of strong electron correlation in these materials, in essence meaning that the Coulomb repulsion among electrons needs to be taken into account with some care. Continuum quantum Monte Carlo (QMC) methods[2] have the potential to address this need, as they are capable of taking the many body correlations of interacting electrons explicitly into account with few fundamental approximations. Though the application of such methods generally comes at a high computational cost, with the dramatic increase in available computing power seen in recent years these methods are now being brought to bear[3–9] on this challenging class of materials.

One of the most prominent approximations involved in the practical application of quantum Monte Carlo techniques is the use of pseudopotentials to remove the high-energy core electrons. The fundamental idea behind pseudopotentials is that they preserve the electronic characteristics of the valence bonding region while shielding calculations from the cost of including the relatively less responsive core electrons. Validation of candidate pseudopotentials therefore naturally involves a (necessarily limited) set of quantitative tests of valence energetics in different environments against exact expectations. The development of and validation of accurate and efficient pseudopotentials therefore comprises an important part of QMC practice.

Several efforts have been made to date within the QMC community to obtain pseudopotentials of good quality for transition metal species. Early atomic calculations of Sc, Ti, Mn, Fe, and Cu by Mitas[10] showed that substantial errors could be encountered if the pseudopotential core was too large. A subsequent study[11] utilizing a more conservative Ne core pseudopotential for Fe showed considerable improvement. A later QMC study by Lee[12] for the Ti atom confirmed these findings for a wide selection of available pseudopotentials. All of the larger core potentials studied demonstrated an error larger than 0.8 eV for at least one ionization potential. Only the neon core Hay-Wadt[13] pseudopotential showed consistent accuracy. More recently, pseudopotential databases covering large portions of the periodic table have been developed. First Trail and Needs[14] published an extensive pseudopotential set covering H-Ba and Lu-Hg in 2005. The pseudopotentials of this set for Sc-Zn are available[15] in large (Ar) and intermediate (Mg) core formats and we are not aware of detailed tests performed within QMC for these potentials. Tests within CCSD(T) of the Mg core pseudopotentials for Sc-Fe have recently been performed as part of a broader effort to create Ne core pseudopotentials for Sc-Zn from multiconfigurational Hartree-Fock calculations[16]. Soon after the original work of Trail and Needs, Burkatzki, Filippi, and Dolg also published Hartree-Fock[17,18] based pseudopotentials for main group elements[19] and then for Sc-Zn[20] with Ne cores. For the second set, ionization potentials and dimer properties were tested within QMC and CCSD(T)[21–23] for Sc and Ti. Similar tests were also performed for another set of Hartree-Fock potentials for

Sc-Mn by Wagner and Mitas[24].

Essentially all transition metal pseudopotentials developed in past efforts have been represented in the Gaussian basis sets prevalent in the quantum chemistry community. For condensed phase studies, it is often convenient to work in the plane wave representation due to straightforward systematic basis set convergence (*i.e.* by increasing the planewave energy cutoff) and the existence of a computationally efficient B-spline representation[25] of the single particle orbitals for QMC calculations.

In this study, we address the absence of transition metal pseudopotentials created with the planewave basis set in mind by developing a new set of potentials for the early row elements Sc-Zn. Our neon core pseudopotentials are based on the local density approximation[26,27] (LDA) of density functional theory[28,29] (DFT) and include scalar relativistic effects. The LDA functional has previously been successfully used to produce a quality Zn pseudopotential for GW[30] calculations[31,32]. A recent work involving some of the authors of this study also confirmed this for Cu[8]. The non-local core radii of our pseudopotentials are restricted to less than 1 a.u. for transferability.

As there is not yet a standard method for creating pseudopotentials solely within QMC, testing pseudopotentials developed with other theories (such as Hartree-Fock or DFT as is standardly done) directly with QMC becomes particularly important. The valence environments we have considered include the behavior of each transition metal (M) atom under successive ionization (from charge states 0 to 4+) and the variation in binding experienced by a M-O dimer under compression and extension. We also compare our computed dimer properties to other bulk DMC calculations using the same pseudopotentials in the recent literature including three transition metal oxides (FeO, NiO, ZnO) and two metals (Ti and Zn). To benchmark our QMC results for our atomic and dimer test cases, we turn to already available highly accurate experimental measurements and high quality quantum chemical calculations. In general, we find the quality of the pseudopotentials to be good, as our QMC results compare favorably with past QMC studies as well as the experimental and theoretical reference data.

The remainder of the paper is organized as follows. In Sec. I we review our approach to constructing pseudopotentials with the widely used OPIUM package[33]. Details regarding the diffusion Monte Carlo (DMC) calculations performed to test the pseudopotentials can be found in Sec. II. We then discuss in Sec. III the results of our atomic and dimer tests in comparison with past DMC studies, benchmark quantum chemical calculations, and experimental results. In Sec. IV we summarize our conclusions. The pseudopotentials themselves are available in the supplemental material in formats compatible with the Quantum Espresso DFT package[34] and the QMCPACK code[35].

I. PSEUDOPOTENTIAL CONSTRUCTION

All of the pseudopotentials presented in this study (Sc-Zn) were generated with the OPIUM package[33] following a uniform strategy. Electronic correlation was treated within the local density approximation (LDA) of DFT and scalar relativistic effects were included. As previous studies have found that semicore effects are pronounced for Ar-core pseudopotentials of these elements, we have opted to remove 10 electrons from the core of each atom (Ne-core) similar to the Burkatzki-Filippi-Dolg pseudopotential set[20]. We choose to include only s, p, and d channels in the pseudopotentials as prior studies have found this to be sufficiently accurate for third row transition metal species[13,14,20,36,37]. We did not explicitly test the effects of adding an f-channel as was done in Ref. 69. The nonlocal cutoff radii for the s, p, and d channels were kept fairly tight at 0.8 a.u., which has previously found to be useful in GW[30] calculations of bulk ZnO[31,32]. The p-channel was selected as the local channel to avoid ghost states.

The reference state for each atom was selected to minimize the deviation between all electron and pseudopotential LDA total energies for a selection of valence configurations: the neutral state, a single electron removed from the 3d shell, a single electron removed from the 4s shell, two electrons removed from 3d, two electrons removed from 4s, and one electron removed from each of 3d and 4s (obviously some configurations do not universally apply, *e.g.* the 3d shell of neutral Sc only has one electron). Optimal reference states selected in this way tended to be more positively charged, with reference pseudo-atoms typically falling in charge states near 3+ or 4+.

The pseudopotentials were cast in both the Troullier-Martins[38] (TM) and "optimized"[39] (OPT) forms. The potential for each angular momentum channel differs somewhat between the two forms. Since diffusion Monte Carlo calculations may show different sensitivities than DFT to pseudopotential details (*e.g.* due to the locality approximation[40]), agreement between DMC test quantities for the two forms serves as an additional quality check. Where such agreement is apparent–as is generally the case in the present study–the optimized form should be preferred as these pseudopotentials have been softened to the extent possible. The planewave cutoff energies required for 1 meV/electron accuracy in DFT (as reported by OPIUM) are shown in table I. These cutoff energies were used throughout the study when generating orbitals within DFT.

We estimate that the optimized pseudopotentials offer a memory savings of about 40% for B-spline represented orbitals. Both sets of pseudopotentials are, however, nearly equally efficient in terms of runtime due to the uniform time access of the B-spline representation. The use of Ne core rather than Ar core pseudopotentials offers a substantial increase in accuracy, but also increases cost (the cost scales like $Z_{eff}^{3.4,41}$). In the case of the Fe atom, for example, the cost increase is around a

	Z_{eff}	Troullier -Martins	Optimized
Sc	11	387	276
Ti	12	370	265
V	13	363	261
Cr	14	364	266
Mn	15	372	269
Fe	16	379	272
Co	17	386	276
Ni	18	389	280
Cu	19	390	280
Zn	20	390	282

TABLE I: Effective core charges (Z_{eff}) and DFT planewave energy cutoffs in Rydbergs to obtain convergence errors below 1 meV/electron for both the Troullier-Martins and optimized pseudopotentials for Sc-Zn.

factor of 10.

II. DMC METHODOLOGY

Diffusion Monte Carlo[42,43] (DMC) calculations are many body in nature and give an accurate account of correlation effects. As the method has been described in detail elsewhere[2], we will only give a sketch of the main features relevant to the current investigation. In DMC, the exact many-body ground state (Ψ_0) and its energy (E_0) can be obtained in the long time limit by applying a projection operator to any trial wavefunction (Ψ_T) provided it has a component on the ground state:

$$\Psi_0 = \lim_{t\to\infty} e^{-t\hat{H}}\Psi_T. \quad (1)$$

Here $\hat{H} = \hat{T}_e + \hat{V}_{ee} + \hat{V}_{eI}$ is the many-body Hamiltonian, including the electron kinetic energy ($\hat{T}_e$), the electron-electron Coulomb interaction $\hat{V}_{ee}$, and the electron-ion interaction $\hat{V}_{eI}$ which may include pseudopotentials.

This projection operation (operator multiplication) can be cast as a path integral in the coordinates of all the electrons, which can be efficiently evaluated as a branching random walk of Monte Carlo electron configurations. The mapping to Monte Carlo integration requires that part of the integrand can be thought of as a probability distribution, requiring a constraint on the projector for practical calculations of fermion systems due to the sign problem. This constraint, the fixed node approximation[43,44], requires that the nodes of trial state remain unchanged by the projection, or $\Psi_T = 0 \Rightarrow \Psi_0 = 0$. This introduces a typically small variational error in the total energy.

When pseudopotentials are used, as in this study, an additional approximation must be made to avoid a second sign problem involving the projector, since it is not guaranteed to be positive definite for non-local operators. In this case, the pseudopotential can either be "localized"[40] by the many-body trial state or sampled with specially developed Monte Carlo moves[45] (T-moves). Each of these approaches introduces an error that vanishes as the trial state approaches the exact ground state, so it is important to use optimized trial wavefunctions. Other errors incurred from necessary approximations regarding the projector that are more straightforward to control include timestep discretization and dynamic control of walker branching (population control).

The QMCPACK[35] simulation code was used for all wavefunction optimization[46], variational[47], and diffusion Monte Carlo[42,43] calculations. We employed the standard Slater-Jastrow form of the trial wavefunction in all calculations, where the nodes are determined by a product of determinants for up ($D^\uparrow$) and down ($D^\downarrow$) spin electrons and a Jastrow factor[48] (J) is used to explicitly model correlations:

$$\Psi_T(R) = e^{-J(R)} D^\uparrow(R^\uparrow) D^\downarrow(R^\downarrow) \quad (2)$$

Here R represents the spatial coordinates of all electrons and $R^\uparrow/R^\downarrow$ refer to coordinate sub-partitions relating to the up or down electrons only. A trial wavefunction of this form has been successfully used to represent transition metal oxides in previous studies[3–6,8,9,20,24] and we find it to be of sufficient accuracy to assess the quality of the present pseudopotentials.

Density functional theory calculations were performed with the Quantum Espresso package to generate single particle orbitals populating the determinants in Eq. 2. For each transition metal (M) atom or M-O dimer, the "total magnetization" ($N_{up} - N_{down}$) was constrained to match the known multiplicity of the state (here N_{up}/N_{down} refer to the number of up/down electrons). Term symbols containing the multiplicity information are included in tables II and III in Sec. III. All DFT calculations were performed in periodic boundary conditions with a simulation cell 15 Å on a side to minimize image effects. In the subsequent QMC calculations with QMCPACK, open boundary conditions were used. The full set of DFT calculations was first performed with LDA. For a few atoms in low charge states, the HSE[49,50] functional was found to give an improvement in the nodes and the first ionization potential. All atomic results reported here are for HSE orbitals. The molecular results were obtained with LDA orbitals.

The linearized[46] optimization method was used to optimize one- and two-body terms in the Jastrow factor. Each DMC calculation was performed with 2048 walkers to minimize population control bias. A conservative timestep of 0.0025 Ha^{-1} was sufficient to converge energies to an accuracy better than the statistical error bars. Both T-moves[45] and the locality approximation[40] were considered for the treatment of non-local pseudopotentials in DMC. This choice amounted to a small change in the ionization potentials (about 0.05 eV). The results quoted throughout the remainder of the paper were calculated with the T-move approach.

III. RESULTS AND DISCUSSION

The Troullier-Martins (TM) and softer optimized (OPT) pseudopotentials were tested by performing diffusion Monte Carlo (DMC) calculations for each transition metal species, M ∈ Sc-Zn, in atomic, dimer, and condensed environments. In the atomic tests, the valence space was varied by successively removing electrons. For each metal atom and pseudopotential form (TM or OPT), five separate DMC calculations were performed, one for each charge state (q) from neutral to 4+. The first through fourth ionization potentials, for which there is generally good experimental data[51], were directly calculated by the total energy differences

$$IP_{q+1} = E^{DMC}_{q+1} - E^{DMC}_{q} \tag{3}$$

with $0 \leq q \leq 4$. The atomic results are summarized in Sec. III A and compared to prior DMC calculations and benchmark experimental data.

The pseudopotentials were tested further by considering the response of transition metal-oxygen (M-O) dimers to compression and extension. Since the spherical symmetry is broken in a dimer, and only the cylindrical symmetry remains, the wave function must hybridize angular momentum components of the original atomic wavefunction to form a bond. The formation of a dimer bond is therefore a strong test of the accuracy the angular momentum decomposition of a given pseudopotential. An accurate prediction of the binding energy and the vibrational frequencies for a dimer should be a strong indication of the pseudopotential effectiveness and transferability for the description of different oxides.

DMC total energies were obtained for each M-O dimer and pseudopotential form (TM or OPT) at nine equally spaced bond distances between 10% compressed and 10% stretched relative to the experimental geometry. Binding curves were obtained by performing a Morse potential fit to the data. Prior to fitting, the dimer data were shifted by the total energy of the isolated M and O atoms. The analytic form of the Morse potential fits,

$$V_{Morse}(r) = D_e \left(1 - e^{-a(r-r_e)}\right)^2, \tag{4}$$

provides access to derived quantities, such as the dimer dissociation energy (D_e), equilibrium bond length (r_e), and vibration frequency ($\omega_e = \frac{a}{\pi c}\sqrt{\frac{D_e}{2\mu}}$, μ = reduced mass) which is related to the zero point vibration energy. Statistical error bars for these quantities were obtained by performing a jack-knife[52] analysis on the Morse potential fits, which essentially amounts to repeated refits using subsets of the energy data. The dimer results are discussed in detail in Sec. III B in comparison to benchmark experimental and high-level quantum chemical calculations. In total, approximately 300 DMC calculations were required to obtain the ionization potentials and dimer binding curves for all the transition metal species with each of the two pseudopotential forms (TM and OPT). A recently developed workflow automation tool was used for this purpose[53].

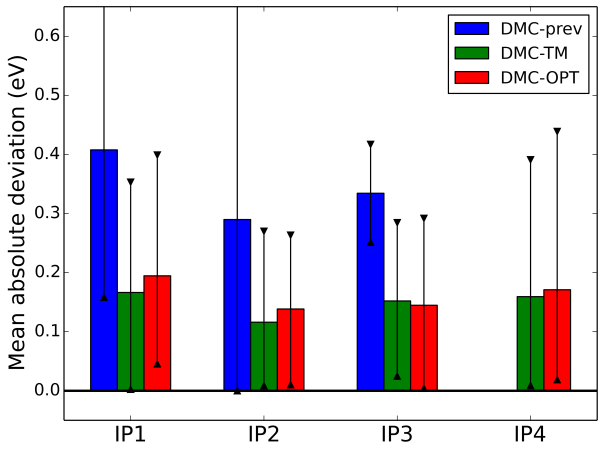

FIG. 1: Comparison of our DMC ionization potential (IP) results (DMC-TM/OPT) with prior DMC work (DMC-prev). Bar heights show mean absolute deviations across Sc-Zn relative to experiment for each IP (IP1-4). Triangles denote the min and max absolute deviations across the same set. Refer to Table II for max values falling outside the visible range.

In the sections that follow we will make extensive use of summarized data in the form of averages in addition to discussing individual data points for a particular metal species and/or quantity. Most often, averages for a particular quantity ($Q \in IP_q, D_e, r_e, \omega_e$) will be taken over atomic species (Sc-Zn). In this case the mean absolute deviation (MAD) from a set of reference data gives a sense of the overall accuracy, while the mean deviation (MD) gives an indication of systematic bias:

$$MAD(Q) = \frac{1}{N_{Sc-Zn}} \sum_{i \in Sc-Zn} |Q^{DMC}_i - Q^{Expt.}_i|$$
$$MD(Q) = \frac{1}{N_{Sc-Zn}} \sum_{i \in Sc-Zn} \left(Q^{DMC}_i - Q^{Expt.}_i\right) \tag{5}$$

The set over which the average is taken will vary as appropriate during the discussion, but the main idea is the same and the set will always be noted. Since averages have a tendency to reduce the visibility of outliers (max or min deviation), these are also noted individually.

We are mainly interested in the overall performance of the pseudopotentials within DMC (referring to prior studies to gauge relative accuracy) and whether the softer optimized pseudopotentials (OPT) and the Troullier-Martins (TM) potentials perform similarly well. As noted earlier, this has a direct impact on their usefulness for condensed phase QMC studies of transition metal oxides that employ the widely used and efficient B-spline representation for orbitals.

A. Atomic properties

Absolute deviations of our DMC ionization potential (IP) results relative to experiment are summarized in Fig. 1. The bars show the MAD across Sc-Zn for each IP for TM and OPT pseudopotentials and also previous DMC studies. The triangles above/below the MAD show the outliers, *i.e.* the max/min absolute deviations. The overall quality of the obtained ionization potential results is quite good, with the two pseudopotential sets showing near identical performance. In the discussion that follows, we state results only for the OPT pseudopotentials for simplicity. In essentially all cases the TM pseudopotentials performed as well or slightly better than the OPT ones.

The full MAD from experiment across all transition metals (Sc-Zn) and ionization potentials (IP1-4) is 0.16(1) eV, while the MD is nearly unbiased at -0.06(1) eV. The maximum deviation is 0.44(3) eV. The MAD's (across Sc-Zn) of the individual IP's are consistently good at 0.20(1) eV or less for IP1 to IP4. However, some systematic bias can be seen from the MD of individual IP's. The first and second IP's tend to be underestimated with a MD across Sc-Zn of -0.16(1) eV, while the fourth IP tends to be overestimated with a MD of 0.11(1) eV. Prior DMC studies also tend to underestimate the first IP with a MD of -0.36(1) eV, while there is little comparative data available for fourth IP's. Both the mean and max absolute deviations are somewhat better for the current study than past investigations, taken as a whole. It should be noted however that the comparison is necessarily limited as the majority of prior DMC data is for the lightest elements, *i.e.* Sc and Ti. The full set of calculated IP's with data shown explicitly for each atom can be found in Table II along with data from prior DMC studies and experimental reference data.

Out of all 40 IP's calculated here only a few show deviations from experiment larger than 0.3 eV: Sc IP4, V IP1, Mn IP4, and Fe IP1. Though occasional deviations like these are not particularly worrisome, it is worth investigating the possible sources of these discrepancies. For the first IP of Fe, we calculated a value of 7.50(4) eV. This deviates from the experimental value[51] of 7.902 eV by -0.40(4) eV. This deviation likely has a large component of fixed node error; of all the IP's, the first IP of Fe showed the greatest sensitivity to the choice of nodes (LDA or HSE). Our results also compare well with the pioneering work of Mitas[11] (7.67(6) eV) and the more recent work of Buendia, *et al.*[54] (7.55(2) eV), where at least one additional excited state determinant was included. The deviation seen for the fourth IP of Mn (0.36(3) eV) may be real, but also might reflect a lack of precision in the available experimental data. The data for the fourth IP's of Mn-Ni are given with a probable uncertainty of 0.1 eV or more[55].

The deviations seen for the lighter elements (Sc IP4 and V IP1) may be more surprising at first glance than those for the heavier elements, which are naturally expected to be more challenging. The deviation observed for Sc IP4 is the largest in the set at 0.44(3) eV from experiment for, however the cause is fairly obvious: this IP is also the only one that depopulates the 3p subshell. The experimentally observed IP is 73.489 eV, fully 30 eV larger than the 4th IP of Ti that removes the last 3d electron. The first IP of V, by contrast, is among the least energetic experimentally at 6.746 eV and we find 6.42(4) eV within DMC. While most of the first IP's along the row involve a direct depopulation of the 4s subshell (*i.e.* $3d^n4s^m \rightarrow 3d^n4s^{m-1}$), for V (along with Co and Ni) the transition involves a change in occupation of both 3d and 4s ($3d^n4s^2 \rightarrow 3d^{n+1}$), which can be thought of as a 4s→3d excitation followed by a removal of the remaining 4s electron. The relatively challenging nature of these ionization potentials has been observed before in high-level quantum chemical calculations[56] and also appears to be a factor in the recent DMC study of Ref. 54. There, fairly large errors were seen for the first IP of V (-0.60(2) eV), Co (-0.71(3) eV), and Ni (-0.82(3) eV) while the MAD for the remaining seven elements was only 0.30 eV[54]. Though the deviation seen in this study for V IP1 (-0.33(4)) is somewhat above the average of 0.2 eV, the other two elements undergoing a similar transition show consistent behavior (-0.22(5) eV for Co and -0.23(4) eV for Ni).

B. Dimer properties

The binding properties of transition metal-oxygen (M-O) dimers provide an additional test of our pseudopotentials. Quantities derived from Morse potential fits to DMC binding data of M-O dimers can be found in Figure 2. As in Figure 1, each column denotes the mean absolute deviation from experiment across ScO-ZnO for each group of theoretical results and the outliers in each set are represented by triangles. Note that prior DMC data is not available for the heavier elements (FeO-ZnO). In addition to displaying DMC results from the present (DMC-TM/DMC-OPT) and prior (DMC-prev) studies[20,24,57], Figure 2 contains reference data from high-level quantum chemical calculations[58–64], including multi-reference configuration interaction at the level of singles and doubles excitations (denoted MRCI or MRCI+Q with a Davidson-like correction), and restricted/unrestricted coupled cluster with singles, doubles, and perturbative triples (RCCSD(T)/UCCSD(T)). In the discussion below, the deviation from experiment of these three quantum chemical methods is expressed as a range rather than three separate and individually labeled numbers for brevity. The full set of data resolved for each dimer is available in Table III. Overall, both the Troullier-Martins and optimized pseudopotentials perform well in absolute terms and are comparable to prior DMC studies and quantum chemical reference calculations.

The bond lengths derived from our DMC binding data

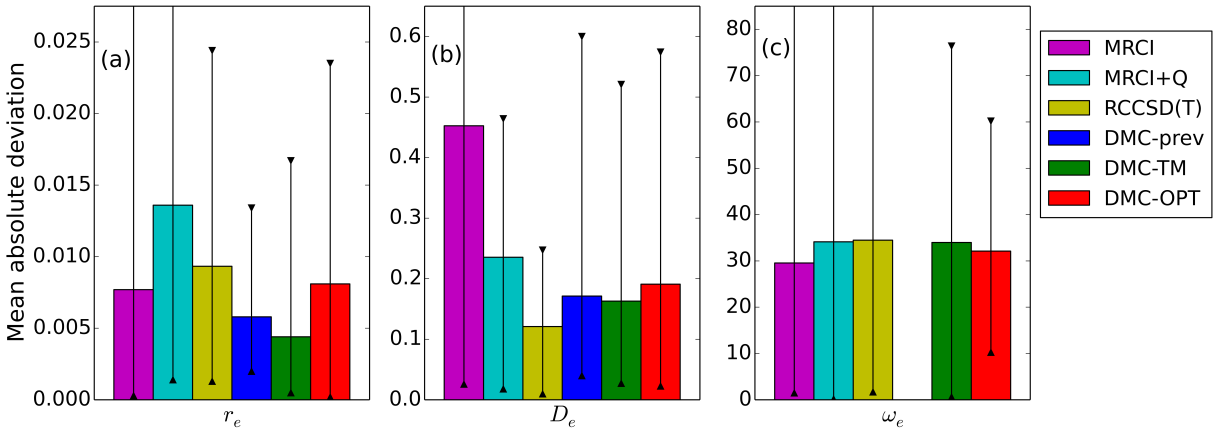

FIG. 2: Comparison of our DMC dimer results (DMC-TM/OPT) with prior DMC work (DMC-prev) and quantum chemical methods (MRCI, MRCI+Q, and RCCSD(T). Bar heights show mean absolute deviations across ScO-ZnO relative to experiment for each dimer quantity: (a) r_e in Å, (b) D_e in eV, (c) ω_e in cm^{-1}. Triangles denote the min and max absolute deviations across the same set. Refer to Table III for max values falling outside the visible range.

are generally in very good agreement with the experimental reference data and with prior DMC and quantum chemical calculations. The MAD from experiment across ScO-ZnO is just 0.008(1) Å for our pseudopotentials and the MD is 0.003(1) Å. This corresponds to an accuracy of 0.5(1)% on average, though the performance is not uniform along the row (the maximum deviation is 1.4(2)%). For ScO-MnO, prior DMC results are available[24] and recent quantum chemical calculations[58,59] perform very well. Here all studies are similarly accurate with relative MAD's of 0.4(1)% (this work), 0.4% (DMC of Ref. 24), and 0.1-0.3% (quantum chemistry[58,59]). For FeO-NiO, somewhat larger errors were observed for the quantum chemical approaches[60–62] (0.9-1.7%) while similar accuracy was maintained in DMC (0.3(1)%). The most challenging dimers overall were the weakly bound CuO and ZnO. For CuO we find the largest deviation with a relative error of 1.4(2)% compared to 2.7% for the only available RCCSD(T) study[63]. Finally for ZnO, our calculations give a relative error of 0.7(2)% for the bond length, comparable to RCCSD(T)[64] (0.8%). Overall both pseudopotential sets perform well, with bond lengths generally in agreement with experiment to better than 1%.

The dissociation energies across the row decrease nearly monotonically with increasing Z, showing strong (ScO-VO), moderate (CrO, MnO-NiO), and relatively weak (CuO and ZnO) binding. With the exception of CrO, our calculated bond dissociation energies are in good agreement with experiment. For all the numerical values that follow, error bars quoted include the experimental uncertainty, where provided. The accuracy we find for D_e with our pseudopotentials (MAD of 0.19(2) eV, CrO excluded) is consistent with what has been observed for the IP's. In general, the bond dissociation energies are underestimated with a MD of -0.16(2) eV, which is also most often the case for previous DMC studies. For the strongly bound molecules (ScO-VO), all DMC studies show nearly identical accuracy for D_e with MAD's of 0.08(4) eV (this work) and 0.09(4) eV (Refs. 24,20). As anticipated, the quantum chemical approaches[58,59] are more accurate with MAD's of 0.03(4)-0.06(4) eV. For the moderately bound molecules (MnO-NiO) our DMC results (MAD of 0.16(3) eV) are competitive with the quantum chemical results[58,60–62] (MAD's of 0.18(3)-0.71(3) eV). For the least strongly bound molecules, our performance is mixed with absolute deviations of 0.31(2) eV for CuO and 0.16(4) eV for ZnO. Prior RCCSD(T) studies[63,63] found better agreement, deviating only 0.12 eV for CuO and 0.02(4) eV for ZnO from experiment.

For the case of CrO we observed a large deviation of 0.57(7) eV from experiment. Here the quantum chemical calculations[58] generally perform better with absolute deviations of 0.19(7)-0.60(7) eV. By contrast, Cr is one of the best performers for the IP tests, with a MAD across IP1-4 of just 0.09(2) eV. Our result for the binding energy of CrO is 4.01(2) eV, which is identical to the D_e of 3.98(2) eV found in the prior DMC study of Ref. 24 with a different Ne-core pseudopotential. Of all the dimers considered in that study (ScO-MnO), CrO showed the greatest sensitivity to the choice of trial wavefunction (Hartree-Fock vs. B3LYP nodes). Given the available evidence, and considering the uniform pseudopotential construction scheme used here, we believe the deviation observed for CrO primarily reflects the limitations of a Slater-Jastrow trial wavefunction rather than a lack of pseudopotential quality.

Consistent with diminishing binding energy, the experimental vibration frequencies generally decrease from ScO to ZnO. Similar to the bulk modulus of solids, dimer

vibration frequencies are extremely sensitive to any errors in the binding curves and a relative accuracy of 5-10% is generally good. The MAD from experiment of our ω_e results for ScO-ZnO is 32(2) cm^{-1}, corresponding to a relative accuracy of about 4%. The results are nearly unbiased with a MD of 11(2) cm^{-1}. The maximum deviation is 76(7) cm^{-1}, or about 9%. The quality of our ω_e results relative to the quantum chemical calculations follows a pattern similar to what has been discussed for the bond lengths and dissociation energies (ω_e data is not available for comparison from prior DMC works). For the early series ScO-MnO, the MAD for DMC is 34(3) cm^{-1} which is near the overall MAD for ScO-ZnO. Over this same range, quantum chemistry[58,59] performs significantly better with MAD's of 4-16 cm^{-1}. For the mid-row FeO-NiO, DMC performs comparatively well with a MAD of 25(4) cm^{-1} (49(4) cm^{-1} for TM) for versus 53-84 cm^{-1} for quantum chemistry[60–62]. Finally, for CuO and ZnO the performance is similar between our DMC work and the available coupled cluster calculations, with absolute deviations of 60(1) cm^{-1} for CuO (68 cm^{-1} RCCSD(T)[63]) and 18(8) cm^{-1} for ZnO (11 cm^{-1} RCCSD(T)[64]). The outliers in our ω_e results are off by about 70 cm^{-1} (approaching 10%), with TM or OPT alternately performing better or worse. We estimate that a deviation of about 0.05 eV across the range of bond lengths used here (10% stretched or compressed) would result in a shift of this magnitude, which is near the limit of accuracy that can be expected of the current DMC calculations.

C. Comparison with bulk studies

The optimized pseudopotentials presented here have also been employed in a few recent studies of bulk transition metal oxides[65–67] as well as bulk metals[65,68]. For comparison with our dimer results, we reproduce the bulk data in Table IV with permission of the authors. Overall, the level of accuracy observed for atomic and dimer properties corresponds well to the representative bulk transition metal oxides (rocksalt FeO, rocksalt NiO, wurtzite ZnO) and metals (hcp Ti, hcp Zn). The average deviation from experiment for the TiO, FeO, NiO, and ZnO dimers is 0.3%, 0.11(2) eV, and 2% for the bond length, dissociation energy, and vibrational frequency, respectively. The average deviation across all bulk systems is 0.3%, 0.15(1) eV, and 4% for the lattice parameters, cohesive energy, and bulk modulus, respectively. The maximum deviations are 0.7%, 0.19(4) eV, and 3% for dimers and 0.5%, 0.34(2) eV, and 8% for bulk systems.

IV. SUMMARY

In summary, we have prepared a set of neon-core pseudopotentials based on LDA for the transition metal elements Sc-Zn for use in quantum Monte Carlo calculations of transition metal oxides. The pseudopotentials were constructed within both the Troullier-Martins and optimized schemes available through the OPIUM pseudopotential generation package in an effort to limit the memory required for a high-fidelity B-spline representation of the resulting single particle orbitals. We have tested both forms of the pseudopotentials directly within DMC in atomic and dimer environments. The atomic and dimer results compare favorably with past DMC studies and benchmark quantum chemical calculations. Atomic ionization potentials, metal-oxygen dimer binding energies, and bulk cohesive energies were all found to be accurate to 0.2 eV on average, or about 5 kcal/mol (max error: 0.6 eV or 15 kcal/mol). Equilibrium dimer bond lengths were found to be chemically accurate, deviating by less than 0.5% from experiment on average (max error: 1.5%). Sensitive dimer vibration frequencies were also found to be well reproduced (mean/max error: 35/76 cm^{-1}). Other recent DMC studies of bulk properties using these pseudopotentials have confirmed the expected level of accuracy in periodic environments. While both the Troullier-Martins and optimized pseudopotentials perform similarly well, the optimized form should be favored due to the reduced memory requirements in QMC. We expect the pseudopotentials developed here to be of use in future quantum Monte Carlo studies of bulk transition metal oxides. The pseudopotentials may also be of interest to practitioners of other correlated many-body methods, such as GW.

Acknowledgements

The authors would like to thank Paul Kent for helpful discussions throughout the development of this study. We would also like to thank Chandrima Mitra and Anouar Benali for providing DMC data for bulk NiO and Ti, respectively. We gratefully acknowledge funding support provided by the Materials Sciences and Engineering Division of the Office of Basic Energy Sciences, U.S. Department of Energy. This research used resources of the Oak Ridge Leadership Computing Facility, which is a DOE Office of Science User Facility supported under Contract DE-AC05-00OR22725.

[1] D. N. Basov *et al.*, Rev. Mod. Phys. **83**, 471 (2011).
[2] W. M. C. Foulkes, L. Mitas, R. J. Needs, and G. Rajagopal, Rev. Mod. Phys. **73**, 33 (2001).
[3] R. J. Needs and M. D. Towler, International Journal of Modern Physics B **17**, 5425 (2003).
[4] L. K. Wagner, Journal of Physics: Condensed Matter **19**,

	Sc	Ti	V	Cr	Mn	Fe	Co	Ni	Cu	Zn	MD	MAD	max	min
	^{2}D	^{3}F	^{4}F	^{7}S	^{6}S	^{5}D	^{4}F	^{3}F	^{2}S	^{1}S				
	3d4s^2	3d^{2}4s^2	3d^{3}4s^2	3d^{5}4s	3d^{5}4s^2	3d^{6}4s^2	3d^{7}4s^2	3d^{8}4s^2	3d^{10}4s	3d^{10}4s^2				
IP1														
DMC-prev	6.40(2)[20]	6.60(3)[20]				7.67(6)[11]				8.5[69]				
DMC-prev	6.40(2)[54]	6.57(2)[54]	6.15(2)[54]	6.52(2)[54]	7.19(3)[54]	7.55(2)[54]	7.17(3)[54]	6.82(3)[54]	7.34(3)[54]	8.98(3)[54]	-0.41(1)	0.41(1)	0.89(3)	0.16(2)
DMC-TM	6.56(3)	6.65(4)	6.39(5)	6.72(4)	7.13(5)	7.59(5)	7.83(5)	7.50(6)	7.59(5)	9.24(5)	-0.17(2)	0.17(2)	0.36(5)	0.00(3)
DMC-OPT	6.51(3)	6.78(4)	6.42(4)	6.65(4)	7.22(6)	7.50(4)	7.66(5)	7.41(4)	7.55(6)	9.23(6)	-0.19(1)	0.19(1)	0.40(4)	0.05(4)
Expt.	6.561[51]	6.828[51]	6.746[51]	6.767[51]	7.434[51]	7.902[51]	7.881[51]	7.640[51]	7.726[51]	9.394[51]				
	^{3}D	^{4}F	^{5}D	^{6}S	^{7}S	^{6}D	^{3}F	^{2}D	^{1}S	^{2}S				
	3d4s	3d^{2}4s	3d^4	3d^5	3d^{5}4s	3d^{6}4s	3d^8	3d^9	3d^{10}	3d^{10}4s				
IP2														
DMC-prev	12.80(2)[20]	13.58(3)[20]								17.1[69]	-0.29(2)	0.29(2)	0.86(3)	0.00(2)
DMC-TM	12.59(3)	13.40(4)	14.58(4)	16.47(4)	15.55(4)	16.12(4)	16.83(4)	17.90(5)	20.26(5)	17.97(5)	-0.11(1)	0.11(1)	0.27(5)	0.01(5)
DMC-OPT	12.54(3)	13.35(4)	14.59(4)	16.56(4)	15.49(3)	16.06(4)	16.87(4)	18.02(4)	20.30(5)	17.82(5)	-0.12(1)	0.14(1)	0.26(3)	0.01(5)
Expt.	12.800[51]	13.576[51]	14.618[51]	16.486[51]	15.64[51]	16.188[51]	17.084[51]	18.169[51]	20.292[51]	17.964[51]				
	^{2}D	^{3}F	^{4}F	^{5}D	^{6}S	^{5}D	^{4}F	^{3}F	^{2}D	^{1}S				
	3d	3d^2	3d^3	3d^4	3d^5	3d^6	3d^7	3d^8	3d^9	3d^{10}				
IP3														
DMC-prev	24.34(2)[20]	27.24(3)[20]									-0.33(2)	0.33(2)	0.42(2)	0.25(3)
DMC-TM	24.82(3)	27.65(3)	29.36(3)	31.12(3)	33.84(3)	30.37(4)	33.27(4)	34.98(4)	36.68(5)	39.75(4)	-0.03(1)	0.15(1)	0.28(4)	0.03(4)
DMC-OPT	24.83(3)	27.65(3)	29.32(4)	31.11(3)	33.79(3)	30.41(4)	33.29(4)	34.90(4)	36.65(4)	39.72(4)	-0.04(1)	0.14(1)	0.29(4)	0.00(4)
Expt.	24.757[51]	27.492[51]	29.311[51]	30.96[51]	33.668[51]	30.652[51]	33.5[51]	35.19[51]	36.841[51]	39.723[51]				
	^{1}S	^{2}D	^{3}F	^{4}F	^{5}D	^{6}S	^{5}D	^{4}F	^{3}F	^{2}D				
	3s^{2}3p^6	3d	3d^2	3d^3	3d^4	3d^5	3d^6	3d^7	3d^8	3d^9				
IP4														
DMC-TM	73.88(3)	43.39(3)	46.87(3)	49.15(3)	51.47(3)	55.00(4)	51.16(4)	54.96(4)	57.16(4)	59.42(4)	0.09(1)	0.16(1)	0.39(3)	0.01(3)
DMC-OPT	73.93(3)	43.38(3)	46.91(3)	49.18(3)	51.56(3)	54.96(4)	51.15(4)	54.95(4)	57.22(4)	59.46(4)	0.11(1)	0.17(1)	0.44(3)	0.02(3)
Expt.	73.489[51]	43.267[51]	46.709[51]	49.16[51]	51.2[51]	54.8[51]	51.3[51]	54.9[51]	57.38[51]	59.4[51]				
	^{2}P	^{1}S	^{2}D	^{3}F	^{4}F	^{5}D	^{6}S	^{5}D	^{4}F	^{3}F				
	3s^{2}3p^5	3s^{2}3p^6	3d	3d^2	3d^3	3d^4	3d^5	3d^6	3d^7	3d^8				

TABLE II: First through fourth ionization potentials (IP1-IP4) in eV for fourth row transition metal atoms Sc-Zn. Term symbols and valence occupations above/below each set of IP data refer to the atomic electronic state before/after ionization. DMC results from this work are labeled DMC-TM for Troullier-Martins and DMC-OPT for optimized pseudopotentials. DMC results from prior studies are labeled DMC-prev with citations listed above each numerical value. All experimental data (Expt.) was taken from Ref. 51. Values in parentheses show the statistical uncertainty in the last digit.

	ScO	TiO	VO	CrO	MnO	FeO	CoO	NiO	CuO	ZnO	MD	MAD	max	min
	$^2\Sigma^+$	$^3\Delta$	$^4\Sigma^-$	$^5\Pi$	$^6\Sigma^+$	$^5\Delta$	$^4\Delta$	$^3\Sigma^-$	$^2\Pi$	$^1\Sigma^+$				
r_e														
MRCI	1.662[58]	1.623[58]	1.588[59]	1.621[58]	1.648[58]	1.606[60]	1.618[61]	1.597[62]			-0.007	0.008	0.030	0.000
MRCI+Q	1.667[58]	1.623[58]	1.591[59]	1.617[58]	1.634[58]	1.594[60]	1.606[61]	1.589[62]			-0.012	0.014	0.038	0.001
RCCSD(T)	1.668[58]	1.619[58]	1.583[59]	1.62[58]	1.645[58]	1.595[60]	1.611[61]	1.606[62]			-0.009	0.009	0.024	0.001
RCCSD(T)	1.680[63]	1.628[63]	1.602[63]	1.634[63]	1.665[63]			1.652[63]	1.771[63]	1.71[64]	0.019	0.019	0.047	0.008
UCCSD(T)	1.679[63]	1.622[63]	1.581[63]	1.621[63]	1.658[63]				1.771[63]		0.011	0.013	0.047	0.000
DMC-prev	1.679(2)[24]	1.612(3)[24]	1.587(3)[24]	1.617(4)[24]	1.652(4)[24]						0.001(1)	0.006(1)	0.013(2)	0.002(3)
DMC-TM	1.665(1)	1.614(1)	1.585(1)	1.625(2)	1.647(3)	1.618(1)	1.624(2)	1.628(1)	1.730(3)	1.688(3)	-0.002(1)	0.004(1)	0.017(3)	0.001(1)
DMC-OPT	1.666(1)	1.614(1)	1.586(1)	1.625(2)	1.668(2)	1.618(1)	1.638(2)	1.625(2)	1.748(3)	1.693(3)	0.003(1)	0.008(1)	0.024(3)	0.000(1)
Expt.	1.666[70]	1.620[71,72]	1.589[73,74]	1.621[75]	1.648[76]	1.619[77]	1.628[78]	1.6271[79]	1.724[80,81]	1.705[82]				
D_e														
MRCI	7.029[58]	6.843[58]	6.509[59]	3.976[58]	3.062[58]	3.408[60]	3.274[61]	3.365[62]			-0.42(2)	0.45(2)	0.81(9)	0.03(7)
MRCI+Q	6.938[58]	6.852[58]	6.578[59]	4.345[58]	3.413[58]	3.716[60]	3.660[61]	3.656[62]			-0.21(2)	0.24(2)	0.46(1)	0.02(1)
RCCSD(T)	6.908[58]	6.813[58]	6.470[59]	4.388[58]	3.716[58]	3.933[60]	3.855[61]	3.981[62]			-0.09(2)	0.12(2)	0.25(1)	0.01(9)
RCCSD(T)	6.9[63]	6.84[63]	6.26[63]	4.3[63]	3.56[63]			3.93[63]	2.66[63]	1.63[64]	-0.11(2)	0.13(2)	0.28(7)	0.02(1)
UCCSD(T)	6.89[63]	6.81[63]	6.04[63]	4.16[63]	3.42[63]				2.66[63]		-0.25(3)	0.25(3)	0.44(9)	0.03(1)
DMC-prev	7.06(3)[24]	6.81(3)[24]	6.54(3)[24]	3.98(2)[24]	3.66(3)[24]									
DMC-prev	7.05(2)[20]	6.91(2)[20]									-0.07(3)	0.17(3)	0.60(7)	0.04(7)
DMC-TM	6.80(2)	6.82(1)	6.57(2)	4.06(1)	3.54(1)	4.25(2)	4.05(1)	3.78(2)	2.54(2)	1.48(2)	-0.13(2)	0.16(2)	0.52(7)	0.03(9)
DMC-OPT	6.79(1)	6.85(1)	6.57(2)	4.01(2)	3.54(2)	4.25(1)	4.00(1)	3.68(2)	2.47(2)	1.45(2)	-0.16(2)	0.19(2)	0.57(7)	0.02(7)
Expt.	6.921(9)[83,84]	6.87(7)[85,86]	6.48(9)[87]	4.58(7)[88]	3.83(8)[89]	4.180[90]	4.08(9)[91]	3.87(3)[92]	2.78[80,93]	1.61(4)[94]				
ω_e														
MRCI	995[58]	1019[58]	1006[59]	897[58]	798[58]	874[60]	893[61]	946[62]			16	30	120	2
MRCI+Q	980[58]	1010[58]	1002[59]	912[58]	842[58]	920[60]	929[61]	974[62]			34	34	148	0
RCCSD(T)	974[58]	1018[58]		910[58]	844[58]	929[60]	926[61]	931[62]			34	34	105	2
RCCSD(T)	971[63]	1014[63]	1028[63]	888[63]	794[63]			874[63]	572[63]	727[64]	-8	28	68	5
UCCSD(T)	973[63]	1080[63]	974[63]	865[63]	779[63]				578[63]		-20	43	71	3
DMC-TM	996(5)	1010(6)	1018(6)	883(8)	790(1)	881(6)	934(6)	902(7)	570(1)	759(9)	7(2)	34(2)	76(7)	1(6)
DMC-OPT	998(5)	1019(6)	1061(6)	851(9)	868(10)	894(5)	910(6)	843(7)	580(1)	756(8)	11(2)	32(2)	60(1)	10(6)
Expt.	975.72[95]	1009.18[71,72]	1001.81[96]	898.5[97]	840.7[98]	882[99]	862.4[100]	825.7[101]	640.17[80,81]	738[82]				

TABLE III: Equilibrium bond lengths (r_e) in Å, dissociation energies (D_e) in eV, and vibration frequencies (ω_e) in cm^{-1} for transition metal dimers ScO-ZnO. As in Table II, the left-most column displays the method used, now including quantum chemical benchmark data (MRCI, MRCI+Q, RCCSD(T), UCCSD(T)) in addition to DMC results from this work (DMC-TM/OPT) and prior studies (DMC-prev). Experimental data (Expt.)[b] follows the selections of the quantum chemical studies[58–64]. Citations are listed above each value and numbers in parentheses show the statistical uncertainty in the last digit.

	FeO	NiO	ZnO	Ti	Zn
a or a, c					
DMC-OPT		4.157(3)[66]	3.245(1), 5.193(1)[65]	2.936(3)[68]	2.656(1), 4.931(1)[65]
Expt.		4.17[102]	3.242, 5.188[103]	2.951[104]	2.664, 4.949[102]
E_{coh}					
DMC-OPT	9.82(1)[67]	9.44(2)[66]	7.42(2)[65]		1.01(2)[65]
DMC-prev	9.66(4)[5]	9.442(2)[3]			
Expt.	9.71[105]	9.5[106]	7.52[107]		1.35[108]
B					
DMC-OPT		196(4)[66]	151.6(4)[65]	106.6(7)[68]	70.2(4)[65]
Expt.		203[106]	140-170[107]	105[109]	60-70[108,110]

TABLE IV: Lattice parameters (Å), cohesive energies (eV), and bulk moduli (GPa) for select bulk materials from other DMC studies employing the optimized pseudopotentials of this work (DMC-OPT), prior DMC studies using other pseudpotentials (DMC-prev), and experiment (Expt.).

343201 (2007).
[5] J. Kolorenč and L. Mitas, Phys. Rev. Lett. **101**, 185502 (2008).
[6] J. Kolorenč, S. Hu, and L. Mitas, Phys. Rev. B **82**, 115108 (2010).
[7] L. Mitas and J. Kolorenč, Reviews in Mineralogy and Geochemistry **71**, 137 (2010).
[8] K. Foyevtsova *et al.*, Phys. Rev. X **4**, 031003 (2014).
[9] L. K. Wagner and P. Abbamonte, Phys. Rev. B **90**, 125129 (2014).
[10] L. Mitáš, in *Computer Simulation Studies in Condensed-Matter Physics V*, Vol. 75 of *Springer Proceedings in Physics*, edited by D. Landau, K. Mon, and H.-B. Schttler (Springer Berlin Heidelberg, Berlin, 1993), pp. 94–105.
[11] L. Mitáš, Phys. Rev. A **49**, 4411 (1994).
[12] Y. Lee *et al.*, Phys. Rev. B **62**, 13347 (2000).
[13] P. J. Hay and W. R. Wadt, The Journal of Chemical Physics **82**, 299 (1985).
[14] J. R. Trail and R. J. Needs, The Journal of Chemical Physics **122**, 174109 (2005).
[15] CASINO Pseudopotential Library, `https://vallico.net/casinoqmc/pplib/`.
[16] J. R. Trail and R. J. Needs, The Journal of Chemical Physics **142**, 064110 (2015).
[17] D. R. Hartree, in *Mathematical Proceedings of the Cambridge Philosophical Society* (Cambridge Univ. Press, Cambridge, 1928), No. 01, pp. 89–110.
[18] V. Fock, Zeitschrift für Physik **61**, 126 (1930).
[19] M. Burkatzki, C. Filippi, and M. Dolg, The Journal of Chemical Physics **126**, 234105 (2007).
[20] M. Burkatzki, C. Filippi, and M. Dolg, Journal of Chemical Physics **129**, 164115 (2008).
[21] K. Raghavachari, G. W. Trucks, J. A. Pople, and M. Head-Gordon, Chemical Physics Letters **157**, 479 (1989).
[22] R. J. Bartlett, J. Watts, S. Kucharski, and J. Noga, Chemical Physics Letters **165**, 513 (1990).
[23] P. J. Knowles, C. Hampel, and H. Werner, The Journal of Chemical Physics **99**, 5219 (1993).
[24] L. K. Wagner and L. Mitas, The Journal of Chemical Physics **126**, 034105 (2007).
[25] D. Alfè and M. J. Gillan, Phys. Rev. B **70**, 161101 (2004).
[26] D. Ceperley and B. Alder, Physical Review Letters **45**, 566 (1980).
[27] J. P. Perdew and A. Zunger, Phys. Rev. B **23**, 5048 (1981).
[28] P. Hohenberg and W. Kohn, Phys. Rev. **136**, B864 (1964).
[29] W. Kohn and L. Sham, Phys. Rev. **140**, A1133 (1965).
[30] L. Hedin, Phys. Rev. **139**, A796 (1965).
[31] H. Dixit, R. Saniz, D. Lamoen, and B. Partoens, Journal of Physics: Condensed Matter **22**, 125505 (2010).
[32] H. Dixit, R. Saniz, D. Lamoen, and B. Partoens, Computer Physics Communications **182**, 2029 (2011).
[33] OPIUM Package, `http://opium.sourceforge.net`.
[34] P. Giannozzi *et al.*, J. Phys. Condens. Matter **21**, 395502 (2009).
[35] J. Kim *et al.*, J. Phys. Conf. Ser. **402**, 012008 (2012).
[36] M. M. Hurley *et al.*, The Journal of Chemical Physics **84**, (1986).
[37] W. J. Stevens, M. Krauss, H. Basch, and P. G. Jasien, Canadian Journal of Chemistry **70**, 612 (1992).
[38] N. Troullier and J. L. Martins, Phys. Rev. B **43**, 1993 (1991).
[39] A. M. Rappe, K. M. Rabe, E. Kaxiras, and J. D. Joannopoulos, Phys. Rev. B **41**, 1227 (1990).
[40] L. Mitáš, E. Shirley, and D. Ceperley, The Journal of chemical physics **95**, 3467 (1991).
[41] B. L. Hammond, P. J. Reynolds, and W. A. Lester, Phys. Rev. Lett. **61**, 2312 (1988).
[42] R. Grimm and R. Storer, J. Comput. Phys. **7**, 134 (1971).
[43] J. B. Anderson, J. Chem. Phys. **63**, 1499 (1975).
[44] J. B. Anderson, The Journal of Chemical Physics **65**, 4121 (1976).
[45] M. Casula, Physical Review B **74**, 161102 (2006).
[46] C. J. Umrigar *et al.*, Phys. Rev. Lett. **98**, 110201 (2007).
[47] W. McMillan, Phys. Rev. **138**, A442 (1965).
[48] R. Jastrow, Phys. Rev. **98**, 1479 (1955).
[49] J. Heyd, G. E. Scuseria, and M. Ernzerhof, The Journal of Chemical Physics **118**, 8207 (2003).
[50] J. Heyd, G. E. Scuseria, and M. Ernzerhof, The Journal of Chemical Physics **124**, 219906 (2006).
[51] W. M. Haynes, *CRC Handbook of Chemistry and Physics. 94th Edition* (CRC Press, Boca Raton, FL, 2013).
[52] B. Efron and B. Efron, *The jackknife, the bootstrap and other resampling plans* (SIAM, Philadelphia, PA, 1982), Vol. 38.
[53] J. T. Krogel, Computer Physics Communications (2015).

[54] E. Buenda, F. Gálvez, P. Maldonado, and A. Sarsa, Chemical Physics Letters **559**, 12 (2013).
[55] W. Lotz, J. Opt. Soc. Am. **57**, 873 (1967).
[56] N. B. Balabanov and K. A. Peterson, The Journal of Chemical Physics **125**, 074110 (2006).
[57] L. Wagner and L. Mitas, Chemical Physics Letters **370**, 412 (2003).
[58] E. Miliordos and A. Mavridis, The Journal of Physical Chemistry A **114**, 8536 (2010).
[59] E. Miliordos and A. Mavridis, The Journal of Physical Chemistry A **111**, 1953 (2007).
[60] C. N. Sakellaris, E. Miliordos, and A. Mavridis, The Journal of Chemical Physics **134**, 234308 (2011).
[61] C. N. Sakellaris and A. Mavridis, The Journal of Physical Chemistry A **116**, 6935 (2012).
[62] C. N. Sakellaris and A. Mavridis, The Journal of Chemical Physics **138**, 054308 (2013).
[63] C. W. Bauschlicher Jr and P. Maitre, Theoretica chimica acta **90**, 189 (1995).
[64] C. W. Bauschlicher and H. Partridge, The Journal of Chemical Physics **109**, 8430 (1998).
[65] J. A. Santana *et al.*, The Journal of Chemical Physics **142**, 164705 (2015).
[66] C. Mitra, J. T. Krogel, J. A. Santana, and F. A. Reboredo, The Journal of Chemical Physics **143**, 164710 (2015).
[67] J. A. Santana, J. T. Krogel, P. R. C. Kent, and F. A. Reboredo, in preparation (2015).
[68] A. Benali *et al.*, in preparation (2015).
[69] W. W. Tipton, N. D. Drummond, and R. G. Hennig, Phys. Rev. B **90**, 125110 (2014).
[70] K. Liu and J. M. Parson, The Journal of Chemical Physics **67**, 1814 (1977).
[71] R. S. Ram, P. F. Bernath, M. Dulick, and L. Wallace, The Astrophysical Journal Supplement Series **122**, 331 (1999).
[72] C. Amiot, P. Luc, and R. Vetter, Journal of Molecular Spectroscopy **214**, 196 (2002).
[73] A. Lagerqvist and L. Selin, Arkiv for Fysik **11**, 429 (1956).
[74] A. Lagerqvist and L. Selin, Arkiv for Fysik **12**, 553 (1957).
[75] P. M. Sheridan, M. A. Brewster, and L. M. Ziurys, The Astrophysical Journal **576**, 1108 (2002).
[76] R. Gordon and A. Merer, Canadian Journal of Physics **58**, 642 (1980).
[77] M. Allen, L. Ziurys, and J. Brown, Chemical Physics Letters **257**, 130 (1996).
[78] S. McLamarrah, P. Sheridan, and L. Ziurys, Chemical Physics Letters **414**, 301 (2005).
[79] R. Ram and P. Bernath, Journal of Molecular Spectroscopy **155**, 315 (1992).
[80] K. Huber and G. Herzberg, *Molecular Spectra and Molecular Structure* (Springer US, New York, 1979), pp. 8–689.
[81] J. W. Baars *et al.*, *Landolt-Börnstein: Numerical Data and Functional Relationships in Science and Technology - New Series* (Springer-Verlag, New York, 1993).
[82] L. Zack, R. Pulliam, and L. Ziurys, Journal of Molecular Spectroscopy **256**, 186 (2009).
[83] P. Luc and R. Vetter, The Journal of Chemical Physics **115**, 11106 (2001).
[84] G.-H. Jeung *et al.*, Phys. Chem. Chem. Phys. **4**, 596 (2002).
[85] H.-P. Loock, B. Simard, S. Wallin, and C. Linton, The Journal of Chemical Physics **109**, 8980 (1998).
[86] D. E. Clemmer, J. L. Elkind, N. Aristov, and P. B. Armentrout, The Journal of Chemical Physics **95**, 3387 (1991).
[87] G. Balducci, G. Gigli, and M. Guido, The Journal of Chemical Physics **79**, 5616 (1983).
[88] R. Georgiadis and P. Armentrout, International journal of mass spectrometry and ion processes **89**, 227 (1989).
[89] S. Smoes and J. Drowart, in *Modern High Temperature Science*, edited by J. Margrave (Humana Press, New York, 1984), pp. 31–52.
[90] D. A. Chestakov, D. H. Parker, and A. V. Baklanov, The Journal of Chemical Physics **122**, 084302 (2005).
[91] F. Liu, F.-X. Li, and P. B. Armentrout, The Journal of Chemical Physics **123**, 064304 (2005).
[92] L. R. Watson *et al.*, The Journal of Physical Chemistry **97**, 5577 (1993).
[93] P. H. Krupenie, Journal of Physical and Chemical Reference Data **1**, 423 (1972).
[94] D. E. Clemmer, N. F. Dalleska, and P. B. Armentrout, The Journal of Chemical Physics **95**, 7263 (1991).
[95] C. L. Chalek and J. L. Gole, Chemical Physics **19**, 59 (1977).
[96] A. Merer, Annual Review of Physical Chemistry **40**, 407 (1989).
[97] W. H. Hocking *et al.*, Canadian Journal of Physics **58**, 516 (1980).
[98] A. Sengupta, Zeitschrift für Physik **91**, 471 (1934).
[99] G. Drechsler, U. Boesl, C. Bäßmann, and E. W. Schlag, The Journal of Chemical Physics **107**, 2284 (1997).
[100] M. Barnes *et al.*, Journal of Molecular Spectroscopy **186**, 374 (1997).
[101] A. Citra, G. V. Chertihin, L. Andrews, and M. Neurock, The Journal of Physical Chemistry A **101**, 3109 (1997).
[102] R. W. G. Wyckoff, *Crystal structures* (Krieger, Malabar, FL, 1964).
[103] J. Albertsson, S. C. Abrahams, and A. Kvick, Acta Crystallographica Section B **45**, 34 (1989).
[104] R. R. Pawar and V. Deshpande, Acta Crystallographica Section A: Crystal Physics, Diffraction, Theoretical and General Crystallography **24**, 316 (1968).
[105] M. W. Chase and National Institute of Standards and Technology (U.S.), *NIST-JANAF thermochemical tables* (American Chemical Society ; American Institute of Physics for the National Institute of Standards and Technology, [Washington, D.C.]; Woodbury, N.Y., 1998).
[106] D. R. Lide, *CRC Handbook of Chemistry and Physics. 75th Edition* (CRC Press, Boca Raton, FL, 1994).
[107] U. Özgür *et al.*, Journal of Applied Physics **98**, 041301 (2005).
[108] C. Kittel, *Introduction to solid state physics* (Wiley, ADDRESS, 2005).
[109] I. Grigoriev, E. Meilikhov, and A. Radzig, Atomizdat, Moscow [in Russian] (1991).
[110] A. Dewaele, M. Torrent, P. Loubeyre, and M. Mezouar, Phys. Rev. B **78**, 104102 (2008).